



Chapter 5: Theory & Modelling of outflows

BAL effect in quasars due to source orientation

M. Sniegowska^{1,2} , M. H. Naddaf^{1,2}, M. L. Martinez-Aldama^{3,4},
P. Marziani⁵, S. Panda⁶ and B. Czerny¹

¹Center for Theoretical Physics, Polish Academy of Sciences,
Lotnikow 32/46, 02-668 Warsaw, Poland
email: msniegowska@camk.edu.pl

²Nicolaus Copernicus Astronomical Center, Polish Academy of Sciences,
Bartycka 18, 00-716 Warsaw, Poland
email: naddaf@cft.edu.pl

³Instituto de Física y Astronomía, Facultad de Ciencias, Universidad de Valparaíso,
Gran Bretaña 1111, Valparaíso, Chile

⁴Departamento de Astronomía, Universidad de Chile, Casilla 36D, Santiago, Chile

⁵INAF-Astronomical Observatory of Padova, Vicolo dell'Osservatorio, 5,
35122 Padova PD, Italy

⁶Laboratório Nacional de Astrofísica - Rua dos Estados Unidos 154,
Bairro das Nações. CEP 37504-364, Itajubá, MG, Brazil

Abstract. We investigated a scenario where the presence of a broad absorption line (BAL) feature in quasars (QSOs) is contingent upon the line of sight being situated within an outflow cone emanating from the source. We examined the mechanism of dust-driven winds based on the failed radiatively accelerated dusty outflow (FRADO) model proposed by Czerny & Hryniewicz, letting it be responsible for the formation of massive outflow. We calculated the probability of observing the BAL effect from the geometry of outflow which is a function of global parameters of black hole mass (M_{\bullet}), Eddington ratio (α_{Edd}), and metallicity (Z). We then compared the results with prevalence of BAL QSOs in a sample of observational data from SDSS. The consistency of our model with the data supports the interpretation of the BAL phenomenon as a result of source orientation, rather than a transitory stage in AGN evolution.

Keywords. Active Galaxies, Broad Absorption Lines, Quasars, Dust, Radiation Pressure

1. Introduction

BAL QSOs represent a unique and enigmatic class of quasars that exhibit prominent blue-shifted absorption features in their spectra (Lynds 1967; Trump et al. 2006) which evidence the presence of strong and massive outflows from the source (Allen et al. 2011; Hamann et al. 2013). They exhibit a continuous and wide absorption trough encompassing velocities reaching several times 10^4 km/s (Risaliti et al. 2005; Gibson et al. 2009). The study of BAL QSOs holds significant importance in understanding the intricate interplay between the accretion disk, black hole, and surrounding environment (Hopkins et al. 2009; Hamann et al. 2019).

BAL QSOs are divided into three types based on the absorption lines present in the spectrum (Hall et al. 2002). High-ionization BAL quasars (HBAL QSOs), constituting approximately 85% of BAL quasars, exhibit absorption features only from highly ionised

atoms. Low-ionization BAL quasars (LBAL QSOs) have high-ionization absorption plus displaying absorption troughs in low-ionisation ions, making up approximately 15% of the entire BAL population. FeLBAL QSOs, the rarest subtype among BAL QSOs, exhibit absorption from both high- and low-ionization species, as well as absorption from Iron excited states.

Observationally, a comparison of multiple wavelengths reveals minimal intrinsic distinctions between BALs and non-BALs, except for the tendency of BAL QSOs to exhibit redder ultraviolet continua compared to non-BAL QSOs (Weymann *et al.* 1991; Lewis *et al.* 2003). BALs are commonly associated with outflows from the accretion disk of active galactic nuclei (AGNs) (Murray *et al.* 1995). The origin of BALs in quasars is subject to two theoretical scenarios. The first suggests that BAL QSOs are essentially normal QSOs observed from a line of sight that passes through the outflowing gas (Elvis 2000). The second scenario involves an evolutionary process (Williams *et al.* 1999) which is no longer preferred (Turnshek 1988). The first scenario relies on the massive outflow of gas due to line-driving mechanism (Elvis 2000; Risaliti *et al.* 2011). However, there are shreds of evidence in the spectra of BAL sources hinting at the presence of dust (Dunn *et al.* 2010; Borguet *et al.* 2013). We, therefore, aimed at testing whether there is any consistency or correlation between the properties of a dust-driven outflow and the probability of observing BAL feature in a given source. For the comprehensive version of this study, see Naddaf *et al.* (2023).

2. Methodology

We use the enhanced 2.5D version of the failed radiatively accelerated dusty outflow model (FRADO) (Czerny & Hryniewicz 2011; Naddaf & Czerny 2022). FRADO model predicts that radiation pressure acting on dust lifts the clumps of dusty material from the surface of an accretion disk. Depending on the launching location and the global parameters, i.e. black hole mass (M_{\bullet}), Eddington ratio (α_{Edd}), and metallicity (Z), the material may then come back to the disk surface or it may escape from the gravitational potential. Also, the launched material may or may not lose the dust content depending on the trajectory (for more details of the 2.5D model, see Naddaf *et al.* 2021; Naddaf & Czerny 2022). An example of the outflow in the 2.5D FRADO model is shown in figure 1 which in this case includes both highly- and lowly-ionized regions shaded in red (dustless) and blue (dusty), respectively. The geometry of the outflow is a function of M_{\bullet} , α_{Edd} , and Z . We calculate the probability of observing BAL feature as

$$P_{\text{BAL}} = \frac{\text{fraction of the sky covered by outflow cone}}{\text{unit sphere}} = \cos(\theta_{\text{min}}) - \cos(\theta_{\text{max}}) \quad (1)$$

As for the observational data, we collected a sample from the quasar catalogue of the Sloan Digital Sky Survey DR7 (Shen *et al.* 2011). The selected sample consists of sources with a median S/N > 10 per pixel in the rest-frame 2700-2900 Å region in which the black hole masses are estimated from MgII λ 2800. The full sample contains 42,349 objects that 3% of which are detected as BAL QSOs. Black hole masses and Eddington ratios for MgII were obtained from the SDSS catalog. Dividing the parameter space of black hole mass and Eddington ratio, M_{\bullet} - α_{Edd} , into bins centered at integer values of $\log M_{\bullet}$ and $\log \alpha_{\text{Edd}}$ with the step size of one in log scale, the median values for the distribution of HBAL and LBAL sources of the sample in each bin are presented in Figure 2. The value from the sample of observational data which can be compared with P_{BAL} from 2.5D FRADO is the *prevalence ratio*, r_{BAL} , defined as

$$r_{\text{BAL}} = \frac{N_{\text{BAL}}}{(N_{\text{BAL}} + N_{\text{nonBAL}})} \quad (2)$$

where N stands for the corresponding number of sources in each bin.

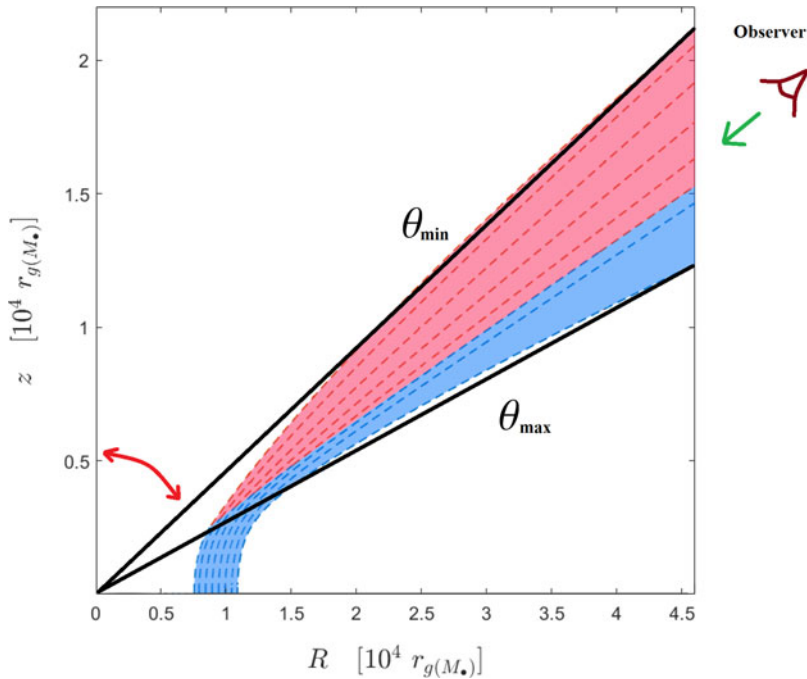


Figure 1. An example of outflow in 2.5D FRADO model for a source at Eddington rate with M_{\bullet} of $10^8 M_{\odot}$ and metallicity of $5Z_{\odot}$. Dotted lines show the path of the trajectory of a clump. The area shaded in blue/red corresponds to the dusty/dustless (lower/higher ionized) actual status of outflowing material. The two black solid lines represent the maximum and minimum angles (to symmetry axis, z) confining the outflow cone. The BAL feature is seen if the line of sight is within the outflow cone.

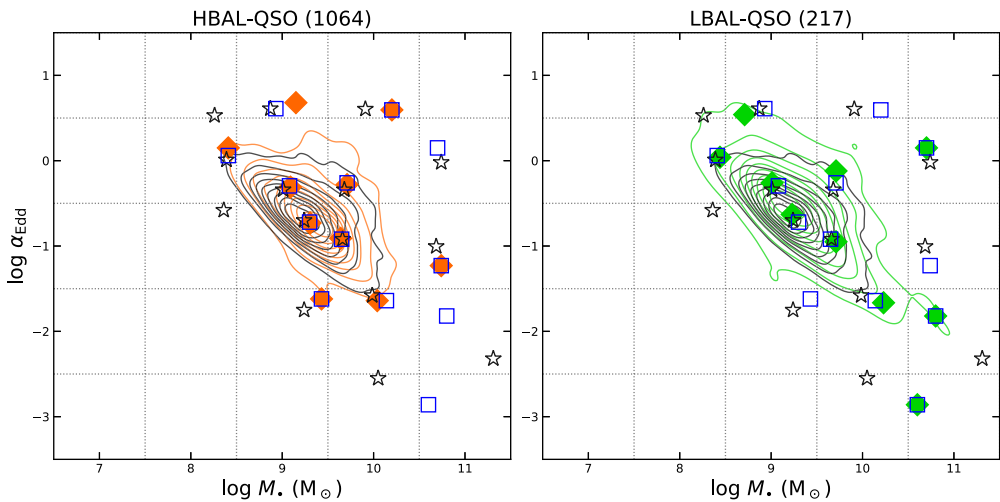


Figure 2. The M_{\bullet} - α_{Edd} space for non-BAL (black \star), BAL (blue \square), HBAL (orange \diamond in the left panel) and LBAL (green \diamond in the right panel) QSOs. Symbols represent the median values of $\log M_{\bullet}$ and $\log \alpha_{\text{Edd}}$ in each bin. Contours in black, orange, and green mark the distribution for non-BAL, HBAL, and LBAL QSOs, respectively.

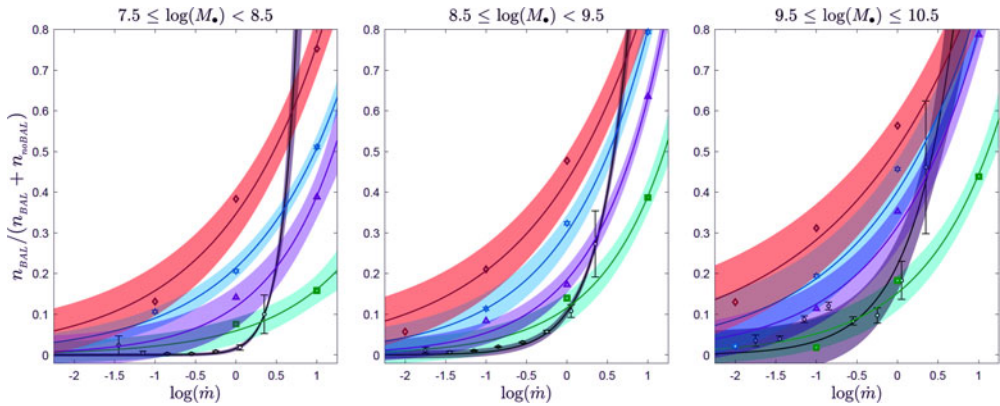


Figure 3. Comparison of r_{BAL} from the sample of observational data with P_{BAL} from 2.5D FRADO, for the range of M_{\bullet} , and α_{Edd} . Solid lines show the best exponential fit to the corresponding data. The values of r_{BAL} and the corresponding fit in each panel are shown in black. Results from 2.5D FRADO, P_{BAL} , for metallicities of 1, 2.5, 5, and 10 Z_{\odot} , and their corresponding fits are color coded in green, violet, blue, and red, respectively.

3. Result & Discussion

Utilizing the 2.5D FRADO model, we obtained the geometry of outflow for a range of global parameters of M_{\bullet} , α_{Edd} , and Z . We then quantified the associated parameter P_{BAL} . Concurrently, we analyzed an observational sample to extract the corresponding r_{BAL} . The figure 3 presents a comparative analysis between the simulation results generated by 2.5D FRADO (colored data points) and observational data (black data points). Remarkably, exponential functions emerged as optimal fits that effectively captured the trends exhibited by the data points in all cases. This striking correlation between theoretical predictions and observational data lends substantial support to the hypothesis that the BAL effect is not a temporary phenomenon but rather arises from the inherent orientation of the source relative to the observer. Specifically, our findings indicate that the BAL effect, both in our model and in the empirical data, is predominantly associated with sources possessing M_{\bullet} exceeding $10^8 M_{\odot}$, and also the effect gets amplified as the accretion rate of the source rises. Here we presented a subset of our results in which the presence of torus is not taken into account for computing the P_{BAL} . In this particular scenario, characterized by the absence of a torus, our analysis reveals a preference for lower metallicities, as evident from the observed trends in the empirical data. However, through further investigations incorporating the torus (see Naddaf *et al.* 2023, for details), we found that higher metallicities are more favored especially when the accretion rate of the source is also higher, as frequently concluded in other studies (see e.g. Martínez-Aldama *et al.* 2018; Panda *et al.* 2019, 2020; Panda 2021; Śniegowska *et al.* 2021; Panda 2022; Garnica *et al.* 2022).

References

- Allen, J. T., *et al.*, *MNRAS* **410**, 2, 860 (2011)
 Borguet, B. C. J., *et al.*, *ApJ* **762**, 1, 49 (2013)
 Czerny, B., Hryniewicz, K., *A&A* **525**, L8 (2011)
 Dunn, J. P., *et al.*, *ApJ* **709**, 2, 611 (2010)
 Elvis, M., *ApJ* **545**, 1, 63 (2000)
 Garnica, K., *et al.*, *A&A* **667**, A105 (2022)
 Gibson, R. R., *et al.*, *ApJ* **692**, 1, 758 (2009)
 Hall, P. B., *et al.*, *ApJS* **141**, 2, 267 (2002)

- Hamann, F., Herbst, H., Paris, I., Capellupo, D., *MNRAS* **483**, 2, 1808 (2019)
- Hamann, F., et al., *MNRAS* **435**, 1, 133 (2013)
- Hopkins, P. F., Murray, N., Thompson, T. A., *MNRAS* **398**, 1, 303 (2009)
- Lewis, G. F., Chapman, S. C., Kuncic, Z., *ApJL* **596**, 1, L35 (2003)
- Lynds, C. R., *ApJ* **147**, 396 (1967)
- Martínez-Aldama, M. L., et al., *A&A* **618**, A179 (2018)
- Murray, N., Chiang, J., Grossman, S. A., Voit, G. M., *ApJ* **451**, 498 (1995)
- Naddaf, M. H., Czerny, B., *A&A* **663**, A77 (2022)
- Naddaf, M. H., Czerny, B., Szczerba, R., *ApJ* **920**, 1, 30 (2021)
- Naddaf, M. H., et al., *A&A* (2023)
- Panda, S., *A&A* **650**, A154 (2021)
- Panda, S., *Frontiers in Astronomy and Space Sciences* **9**, 850409 (2022)
- Panda, S., Marziani, P., Czerny, B., *ApJ* **882**, 2, 79 (2019)
- Panda, S., Marziani, P., Czerny, B., *Contributions of the Astronomical Observatory Skalnaté Pleso* **50**, 1, 293 (2020)
- Risaliti, G., et al., *ApJL* **630**, 2, L129 (2005)
- Risaliti, G., et al., *MNRAS* **410**, 2, 1027 (2011)
- Shen, Y., et al., *ApJS* **194**, 2, 45 (2011)
- Śniegowska, M., et al., *ApJ* **910**, 2, 115 (2021)
- Trump, J. R., et al., *ApJS* **165**, 1, 1 (2006)
- Turnshek, D. A., QSO Absorption Lines, Cambridge Uni. Press (1988)
- Weymann, R. J., Morris, S. L., Foltz, C. B., Hewett, P. C., *ApJ* **373**, 23 (1991)
- Williams, R. J. R., Baker, A. C., Perry, J. J., *MNRAS* **310**, 4, 913 (1999)